Received: 7 November 2018 | Revised: 22 July 2019 | Accepted: 9 September 2019 | Published on: 3 November 2019

DOI: 10.1002/met.1843

RESEARCH ARTICLE

Meteorological Applications RMetS

A method for real-time temporal disaggregation of blended radar–rain gauge precipitation fields

Yannick Barton[1,2,3] | **Ioannis V. Sideris**[3] | **Urs Germann**[3] | **Olivia Martius**[1,2,4]

[1]Institute of Geography, University of Bern, Bern, Switzerland

[2]Oeschger Centre for Climate Change Research, University of Bern, Bern, Switzerland

[3]Federal Office of Meteorology and Climatology MeteoSwiss, Locarno-Monti, Switzerland

[4]Mobiliar Lab for Natural Risks, University of Bern, Bern, Switzerland

Correspondence
Yannick Barton, Hallerstrasse 12, 3012 Bern, Switzerland.
Email: yannick.barton@giub.unibe.ch

Abstract

A fully automated quasi-real-time method is presented to disaggregate hourly to sub-hourly precipitation information operationally in a blended radar–rain gauge product. The method proposes a fully automated solution to disaggregate precipitation in regions characterized by measurement errors or partial absence of auxiliary information on the temporal precipitation evolution. The solution relies on a combination of low-pass filtered radar information and stochastically generated noise fields. A comprehensive validation of the new method is provided demonstrating higher skill compared to a uniform disaggregation in time. The method is now an integral part of CombiPrecip, the official operational code of MeteoSwiss for radar–rain gauge merging.

KEYWORDS

CombiPrecip, disaggregation, geostatistics, meteorological radar, precipitation fields, sub-hourly rainfall

1 | INTRODUCTION

Quantitative precipitation estimates on sub-hourly time scales are of central importance for several research and forecasting applications. They are used, for example, for the (statistical) analysis of short-duration high intensity precipitation events (e.g. Westra *et al*., 2014), as input fields for hydrological modelling of flash flood events (Liechti *et al*., 2013; Smith *et al*., 2014) and for the analysis of mud flow and landslide events (Guzzetti *et al*., 2008; Brunetti *et al*., 2015). Indeed, many of the above applications profit from precipitation information at very short time scales, e.g. 5 min nowcasting applications related to thunderstorms (Panziera *et al*., 2016) or the sector of urban water management for the design and operation of urban drainage infrastructures are specifically highlighted (Urban Rainfall Monitoring, n.d.). The Federal Office of Meteorology and Climatology MeteoSwiss relies on 5 min blended precipitation fields in their operational nowcasting algorithm to generate short-term extrapolations of rainfall quantities over Switzerland used for warnings and for precipitation visualization in the official MeteoSwiss app. The app is viewed by millions of people every day which makes the visual appeal of these precipitation fields a primary concern. However, when blended radar–rain gauge fields are temporally disaggregated to 5 min temporal resolution, artefacts in the precipitation can arise and these need to be mitigated using a fully automatic methodology.

In Switzerland rain gauges provide very accurate measurements of precipitation on the ground; they are too sparsely distributed, however, to capture small-scale high intensity convective precipitation events comprehensively. Radar-based rain estimates fill this gap by providing spatially coherent precipitation estimates at a kilometre scale, that exhibit some biases compared to the rain gauges. CombiPrecip (CPC) is a geostatistical merging scheme that takes advantage of the strengths of both data sources by blending

rain gauge measurements with radar precipitation estimations to produce an optimal estimate of precipitation on a 1 km^2 resolution regular grid over Switzerland (Sideris *et al*., 2014). Technically CPC could perform the blending on any sub-hourly time scale; however, it is operated on hourly aggregations. This is because employing hourly aggregations has the advantages of (a) increasing the modelling stability of the empirical variogram used for the blending process and (b) reducing discrepancies between radar and the rain gauges that arise from various sources of error (Villarini *et al*., 2008; Sideris *et al*., 2014). Hence, the two datasets are merged on longer temporal aggregations (1 hr) and subsequently disaggregated from the hourly time scale to the desired finer sub-period.

A variety of general and rainfall-specific disaggregation methods have been developed since the early 1970s. Koutsoyiannis (2003) provides a comprehensive overview of the strengths and weaknesses of disaggregation methods and discusses several univariate and multivariate stochastic models for coarser and finer time scales. Regarding precipitation, these methods can be summarized into the following four categories with increasing complexity: (a) uniformly distributing higher level data into sub-period data, (b) stochastically generating sub-period data, (c) spatially transferring higher resolution data from a nearby weather station to the area of interest conditional on spatial correlations, and (d) applying a multivariate disaggregation model to combine options (b) and (c) (Debele *et al*., 2007). While these methods succeed at producing artificial series at a finer time scale while conserving the statistical properties of the higher level data, they are not usually designed for generating sub-period data in an unsupervised, real-time fashion and on a national scale. In fact, the few studies (Paulat *et al*., 2008; Wüest *et al*., 2010; Vormoor and Skaugen, 2013; Sideris *et al*., 2014) reporting on generating high resolution sub-daily precipitation data on a regional or national scale use an approach that differs somewhat from those described above.

A commonly used approach to disaggregate high resolution precipitation fields temporally is to consult the temporal patterns of an auxiliary precipitation product with a finer temporal resolution. This auxiliary data product might be biased in absolute terms but it is trusted to provide a realistic and coherent representation of the temporal precipitation evolution at any grid location. For example, Vormoor and Skaugen (2013) provide national-scale daily to 3 hr disaggregation of a daily gridded observational product using the High Resolution Limited Area Model (HIRLAM) precipitation reanalysis data that are available every 3 hr for the temporal disaggregation. Other studies rely on radar precipitation composites. Radar data are ideal for operational quasi-real-time disaggregation since weather radars deliver high resolution information nearly in real time. For example, Paulat *et al*. (2008) and Wüest *et al*. (2010) provide a dataset of daily to hourly precipitation fields using radar composites for Germany and Switzerland. The high temporal resolution and the continuous modernization of the Swiss radar network make radar estimates suitable for disaggregating precipitation accumulations even on sub-hourly time scales. For example, Sideris *et al*. (2014) propose to disaggregate the hourly CPC to 5 min precipitation accumulations for Switzerland.

While this approach is computationally inexpensive, it has one major drawback: it assumes that the temporal evolution of precipitation at each grid location is represented accurately in the auxiliary dataset (here radar precipitation estimates). This may not be the case for grid locations where the radar cannot monitor precipitation with sufficient accuracy. Complex terrains like the terrain in Switzerland typically cause or contribute to such inaccuracies. On some occasions, the blended product CPC may generate positive precipitation accumulations in regions where the radar does not measure any precipitation, and this happens when the rain gauge measurements at the region are different from zero, in the case of limited radar visibility of from smoothing inherent to the blending interpolation scheme. Such inconsistencies are only occasional, but they complicate the disaggregation process, especially in the case of unsupervised real-time applications, leading to artefacts that manifest as sharp gradients in the final sub-hourly precipitation fields.

At locations and time periods where the auxiliary precipitation dataset used for the disaggregation does not provide any information either the final sub-period precipitation field is flagged as missing data (Vormoor and Skaugen, 2013) or the precipitation totals are uniformly distributed across the sub-periods (Paulat *et al*., 2008; Wüest *et al*., 2010). This is appropriate for most types of applications. However, the disaggregated 5 min CPC product is used for real time weather warnings and visualizations of the precipitation in the weather app of the Swiss Weather Service (MeteoSwiss). For this real-time environment both aesthetics and accuracy are at the forefront and this requires a less pragmatic solution to the problem.

In this study a novel method for temporally disaggregating the hourly CPC precipitation product into 5 min precipitation maps is presented that is specifically devised to mitigate artefacts caused by spatial inconsistencies between the blended and radar-only data. The method, fast, flexible and suitable for real-time operational applications, is now an integral part of CPC and can be particularly useful for weather services as an advanced solution for executing disaggregations on their products taking into consideration pragmatic problems such as measurement errors or partial absence of measurements. The sections in this paper are

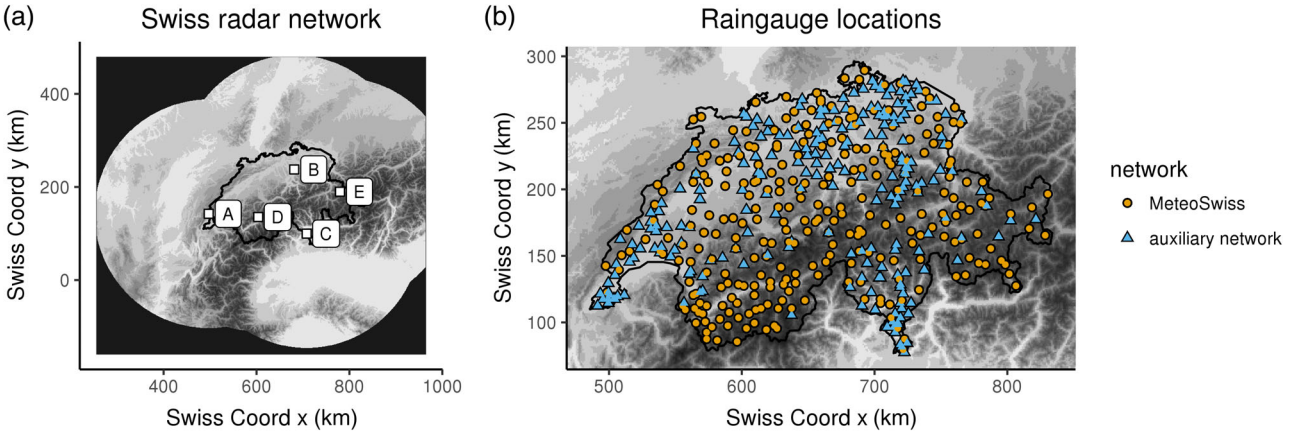

FIGURE 1 (a) The location of the five Swiss radars (A, La Dôle; B, Albis; C, Monte Lema; D, Plaine Morte; E, Weissfluhjoch) along with the radar visibility range (non-darkened region) of the radar composite and CombiPrecip. (b) The location of the rain gauges belonging to the MeteoSwiss and to the auxiliary rain gauge networks in 2017

presented in the following order. First, a brief description of the datasets is given, followed by a detailed presentation of the novel CPC disaggregation method. Then, the verification process of the method is introduced, followed by two illustrative examples to lead finally to a detailed discussion of the results.

2 | DATA

Three datasets are used for the period from 2014 to 2017.

- Five minute radar quantitative precipitation fields obtained from a combination of the five Swiss dual polarization, Doppler, C-band radars are used (see Figure 1a) (Germann *et al*., 2006, 2015). Note that the two latest radars were added to the existing network in 2014 and 2016 to increase the radar visibility in the intra-Alpine regions, affected by orographic shading. The radar estimates, hereafter referred to as AQC, are available for Switzerland and surrounding regions mapped to a 1×1 km regular grid and 5 min resolution. The AQC data provide the temporal and spatial precipitation structures needed for the disaggregation process.
- The basis of all analysis is the hourly blended radar–rain gauge CPC data (Sideris *et al*., 2014). The radar and rain gauge data are merged using co-kriging with external drift to adjust radar estimates with rain gauge observations locally. The automatized merging procedure is performed every 10 min using hourly precipitation aggregations from the current and past hour. The CPC dataset covers the period from 2005 to the present and is available for the same radar domain and at the same spatial resolution as the AQC data. The CPC can be considered as the best estimate of hourly precipitation accumulations at ground in Switzerland.
- An independent set of 10 min rain gauge measurements is used for verification of the disaggregation method, hereafter called the auxiliary network (Figure 1b, orange points). These rain gauges are independent in the sense that they were not involved in the computation of the CPC dataset. Those used to generate the blended CPC data stem from the automatic MeteoSwiss network (Figure 1b, blue triangles). Between 188 and 210 auxiliary stations are used depending on the year. The rain gauges measure precipitation at a 10 min temporal resolution. This auxiliary network comprises rain gauges from MeteoGroup Schweiz AG and cantonal stations (Figure 1b). Note that the coverage of the auxiliary rain gauges is sparse in the inner-Alpine regions. This should have a negligible effect on the verification, however, since the assessment of the disaggregated fields relies on cross-validation (described hereafter).

3 | METHODS

3.1 | Temporal disaggregation method

3.1.1 | The challenge of zero accumulation values in radar-based precipitation estimates

The method proposed here extends the approach presented by Paulat *et al*. (2008), Wüest *et al*. (2010), Vormoor and Skaugen (2013) and Sideris *et al*. (2014). The basic idea is to use 5 min precipitation accumulations at every grid location estimated by the radar (AQC5) to split the hourly CPC accumulations (CPC60) into 5 min accumulations. Hence, for a given hour h the 5 min CPC accumulations (CPC5) at each grid location x are derived by multiplying CPC60 with the corresponding fractions F between AQC5 and the hourly sum of AQC5:

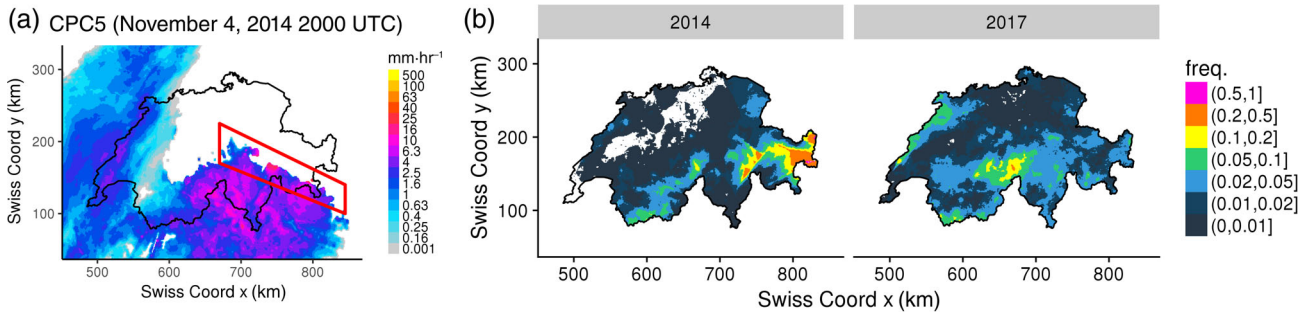

FIGURE 2 (a) An example of a sharp gradient artefact (inside the red rectangle) in the disaggregated 5 min CombiPrecip (CPC) accumulations (CPC5) field of November 4, 2014, 2000 UTC. (b) The fraction of wet hours for which the hourly radar estimates (AQC60) are zero and hourly CPC accumulations (CPC60) are positive in 2014 (left panel) and 2017 (right panel). Thresholds of 0.1 and 0.001 mm·hr^{-1} are used to distinguish between wet and dry time steps in the CPC60 and AQC60 time series respectively

$$\mathrm{CPC5}(x,t_{h,i}) = \mathrm{CPC60}(x,h) \times F(x,t_{h,i}) \quad (1)$$

where $t_{h,i}$ for $i = 1, \ldots, 12$ denotes the 12 5 min time intervals within hour h and the corresponding fractions $F(x, t_{h,i})$ are

$$F(x,t_{h,i}) = \frac{\mathrm{AQC5}(x,\ t_{h,i})}{\sum_{j=1}^{12}\mathrm{AQC5}\left(x,t_{h,j}\right)} \quad (2)$$

The 12 CPC5 values are therefore proportional to the respective 12 AQC5 values and CPC60 is conserved at every location.

A critical limitation of this approach are inconsistencies between the blended and radar-only product, i.e. grid points where CPC60 is positive but the radar does not measure any precipitation and hence all 12 AQC5 values are zero. If this is the case, the division on the right-hand side of Equation (2) cannot be performed and either zero accumulation values or missing data values are assigned to locations where precipitation actually exists. Such inconsistencies may occur in the case of limited radar visibility, from smoothing inherent to the blending interpolation scheme or when the rain gauge measurements at a location where the radar observes no precipitation are different from zero. This can result in sharp spatial precipitation gradients in the final CPC5 images (see Figure 2a). Such artefacts affect mostly light precipitation intensities usually located at the edge of existing precipitation features. They are only occasional (see Figure 2b) and concern mainly intra-Alpine regions where the radar visibility is affected by the topography. Such cases occur in less than 1% of wet hours over the Swiss Plateau and in over 20% in some Alpine regions. It should be noted that, since the two latest Swiss radars have been in operation (2017), spatial inconsistencies between CPC60 and AQC60 have clearly decreased, especially in the eastern Swiss Alps. A more complicated case is when the AQC60 estimate is non-zero at some locations but some of the 12 AQC5 involving this AQC60 show wrongly zero precipitation estimates. Then the disaggregation scheme of Equation (1) disaggregates the CPC60 result wrongly just because it follows the AQC5 precipitation fractions.

3.1.2 | A solution to the zero accumulation problem

A new pragmatic approach is proposed to assign 5 min precipitation fractions F statistically as defined in Equation (22) to grid locations where the radar-based precipitation estimates are zero. Note that the methodology could easily be implemented for 10 min accumulations or for any desired sub-hourly temporal resolution as well. The general idea is to estimate these fractions based on (a) information from nearby grid locations where the radar accumulations are positive and (b) stochastically generated precipitation for grid locations far away from any positive precipitation accumulation in the radar. A new set of 12 AQC5 fields is defined, hereafter called AQC5*, containing non-zero values at every grid location (precipitation accumulations or fractions), which allows an artefact-free partitioning of CPC60 at every grid cell using Equation (1).

The following requirements need to be met in these 12 AQC5* fields. First, CPC60 needs to be conserved at every grid location; therefore, the sum of the fractions over the 12 time sub-periods has to be equal to unity so that the sum of the 12 final CPC5 maps for a given hour is equal to CPC60 of that hour. Second, the fractions have to be constructed in a way that guarantees spatial and temporal continuity of the precipitation fields in the final CPC5 maps. Third, the fractions have to be defined such that they lead to realistic local precipitation structures in the final CPC5 maps. This is relevant because one application of the new dataset may be a visualization of the quasi-real-time precipitation fields in the weather app of the Swiss Federal Office

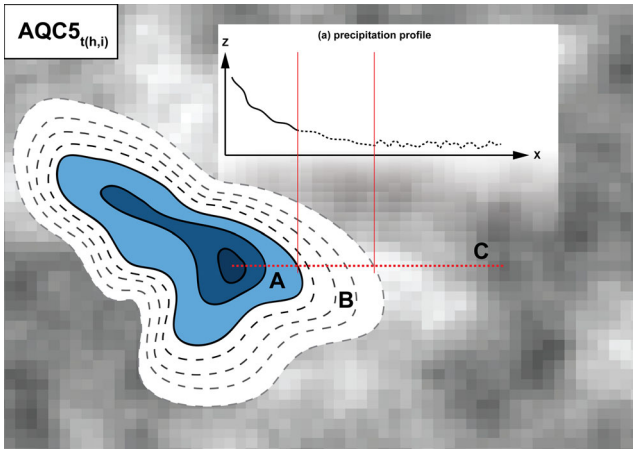

FIGURE 3 Schematic depiction of the new method for one AQC5* ($t_{(h,i)}$). Blue areas (A) indicate locations with actual radar precipitation estimates greater than zero during the last 5 min. For all other locations, where the precipitation estimates are zero, non-zero precipitation values are attributed through dilation (white bands B) and coloured stochastic noise (pixelated region C). The inset shows the precipitation/extrapolated profile (Z) in the direction of X. The extent of area B is determined adaptively according to the rate at which the dilated values converge to the correlated noise C

of Meteorology (MeteoSwiss). Hence, aesthetic requirements are of primary importance and these were checked manually by visualizing a large set of example cases.

The computation of the fractions at grid locations where the radar-based precipitation estimates are zero involves two steps: (i) low-pass filtering of the AQC5 images to dilate the existing precipitation field spatially and (ii) the generation of spatio-temporally correlated noise fields.

Dilation by means of low-pass filtering

The first step consists of dilating the precipitation field in each of the 12 AQC5 fields into regions where no precipitation is observed. This is achieved by iteratively applying a low-pass filter on each of the AQC5 images. For efficiency a filter with a 3×3 pixel kernel is used, where each zero-valued pixel is replaced by the average over the nine grid points. Iterating through this step progressively replaces zeros with non-zero precipitation values that decrease with distance from the observed precipitation with each iteration. The number of iterations is determined adaptively and depends on the rate at which the fractions converge to coloured noise (see below).

The filtering guarantees that the extrapolated AQC5 values seamlessly connect to the edge of the observed radar precipitation and decrease with increasing distance according to the local precipitation gradients (Figure 3, B).

Generation of coloured noise

With increasing distance from the edge of the observed radar precipitation the fractions become independent from the neighbouring non-zero observations as the correlation of the precipitation in space becomes insignificant. At far distance, i.e. once the dilated AQC5 values first reach values smaller than the stochastic values, the fractions are determined stochastically. They are extracted from a sequence of stochastic noise fields with spatio-temporal properties similar to those of precipitation (Figure 3, C). The generation of this stochastic sequence follows Pegram and Clothier (2001) and Berenguer *et al.* (2011), where a sequence of synthetic precipitation fields is obtained by combining autoregressive modelling and spectral filtering in space.

A sequence of 12 temporally correlated Gaussian noise fields $\{Z_t(x)\}$ can be computed using a second-order autoregressive model and is defined as:

$$Z_t(x) = \phi_1 Z_{t-1}(x) + \phi_2 Z_{t-2}(x) + \xi_t(x) \quad (3)$$

where ϕ_1 and ϕ_2 are the model co-efficients and $\xi_t(x)$ is a white noise process in time with mean zero and variance:

$$v^2 = \frac{(1+\phi_2)(1+\phi_1-\phi_2)(1-\phi_1-\phi_2)}{1-\phi_2}$$

Applying Equation (3) repeatedly will produce a sequence of Gaussian noise fields that are temporally correlated and from which 12 fields are retained. The spatial correlation is subsequently imposed by convoluting the 12 temporally correlated fields with a power-law filter with exponent $\beta/2$ (see chapter 4.5 of Pegram and Clothier (2001) for more details). The filtering step is needed at this stage to give more emphasis to lower spatial frequencies than higher spatial frequencies in the noise fields and therefore to create local spatial structures that have a similar autocorrelation structure to real precipitation. The last step consists of applying an exponential transform to the generated fields to obtain positive values at all grid locations and to rescale the fields to the desired variance (preferably very small, i.e. 10^{-7}). Pre-determined values of 0.8, 0.1 and 3 are used for the parameters ϕ_1, ϕ_2 and the $\beta/2$ exponent respectively. These values were found to give appropriate results in mimicking the spatio-temporal properties of precipitation. Whilst in theory these parameters could be estimated in a dynamic manner, they were kept fixed for optimal stability of the disaggregation process.

Linking dilated and stochastic parts

It should be observed that the small background noise is actually added to the dilated precipitation. This does not have any noticeable visual effect on the dilated regions where precipitation is large (since the background correlated noise is small). However, it makes a difference in the smooth transition between dilated regions and noise. This addition

guarantees that the transition is gradual and smooth. Note that for convective precipitation, which by its nature is characterized by steep gradients and low spatial correlations, the fractions F approach the background noise faster. As a consequence the fractions of the hourly CPC60 during convective hours are predominantly determined stochastically. For stratiform precipitation, which by its nature is characterized by more gentle gradients and higher spatial correlations, the fractions converge more slowly to the background noise. As a consequence the fractions of the hourly CPC60 are predominantly conditioned by the transfer of nearby observed information.

Temporal blending (optional)

Performing the temporal disaggregation on successive hourly time intervals can reveal non-negligible temporal discontinuities at the transition of 1 hr to the next in long-term statistical quantities, e.g. a diurnal cycle of average 5 min rainfall. One solution (not discussed within the scope of this work) is to perform the temporal disaggregation from mid-hour to mid-hour (instead of considering the "full hour") and to implement a temporal blending step that aims at temporally linking the 12 disaggregated precipitation values by following a target function (at each pixel location).

3.2 | Verification process of the CPC5 fields

The purpose of the disaggregated data is twofold. First, an operational application in the MeteoSwiss app requires visually convincing precipitation fields and, second, there are quantitative applications such as warning and process studies as well as climatological investigations. These two types of applications require different types of verifications. For the first, the 5 min CPC precipitation fields are assessed by visual inspection (see Section 4.1). For the latter, the verification of the 5 min CPC fields is based (a) on a cross-validation of the CPC5 by artificially blanking (setting to zero) parts of the AQC5 precipitation fields and assessing spatial and temporal properties of those reconstructed parts using the procedure outlined in Section 3.1 and (b) on a comparison of CPC5 values and independent 10 min rain gauge measurements at collocated grid points. The verification is performed on a set of 1,000 carefully selected hours. Only hours for which all Swiss radars were in operation and containing at least 24 wet rain gauges were retained.

The verification is carried out separately for stationary and advective large-scale flow situations, which hereafter are called "slow" and "fast" hours respectively. This allows the assessment of moving precipitation fields, which is of specific interest here, as the disaggregation method presented is expected to account for moving precipitation features. The stratification into slow and fast hours is achieved by extracting the image-mean optical flow in the AQC5 precipitation fields within the respective hour. The optical flow is computed by the correlation-based matching method (Beauchemin and Barron, 1995), i.e. by shifting the current AQC5 field by varying units along the x and y axes and retrieving the largest Pearson correlation co-efficient between the shifted and the fixed antecedent AQC5 field. The 500 hr with the largest hourly average motion are considered as fast (velocity ranges between 13.6 and 46.3 $km \cdot hr^{-1}$) while the 500 hr with the smallest hourly average motion are considered as slow hours (velocity ranges between 0 and 2.4 $km \cdot hr^{-1}$).

Recall that the disaggregation for producing the CPC5 maps relies directly either on the radar-based precipitation accumulations (region A in Figure 3) or on weights estimated by dilation (region B in Figure 3) or stochastically only (region C in Figure 3). Throughout the verification process the distinction is made between locations where the disaggregation is based on radar (A) and extrapolated values (B and C).

A uniform distribution of the precipitation over the 12 sub-hourly (5 min) time intervals is used as a benchmark for assessment of the disaggregation method, similarly to Vormoor and Skaugen (2013). This approach, called the uniform method hereafter, can be considered as the simplest and most pragmatic (e.g. Gutierrez-Magness and McCuen, 2004). Note that it is seldom adapted for most practical applications due to the extremely variable nature of precipitation both in space and time.

For more clarity, the following terminology is introduced and used hereafter. CPC5-UNI refers to CPC data with 5 min resolution after disaggregation using a uniform distribution. CPC5-DIS refers to CPC data with 5 min resolution using the novel disaggregation technique introduced in Section 3.1, and CPC5-REF refers to reference 5 min resolution CPC data of the cross-validation. The rain gauge assessment requires 10 min precipitation aggregations, and therefore AQC10, CPC10-UNI and CPC10-DIS refer respectively to 10 min radar aggregations, CPC data with 10 min resolution after disaggregation using a uniform distribution and CPC data with 10 min resolution using the method proposed in this study.

4 | RESULTS

4.1 | Examples

The disaggregation method is illustrated through two examples representative of a slow and a fast moving precipitation field. The first example (Figure 4) shows quasi-stationary precipitation on November 4, 2014, between 1800 and 1900 UTC in a persistent weak southwesterly flow, a so-called

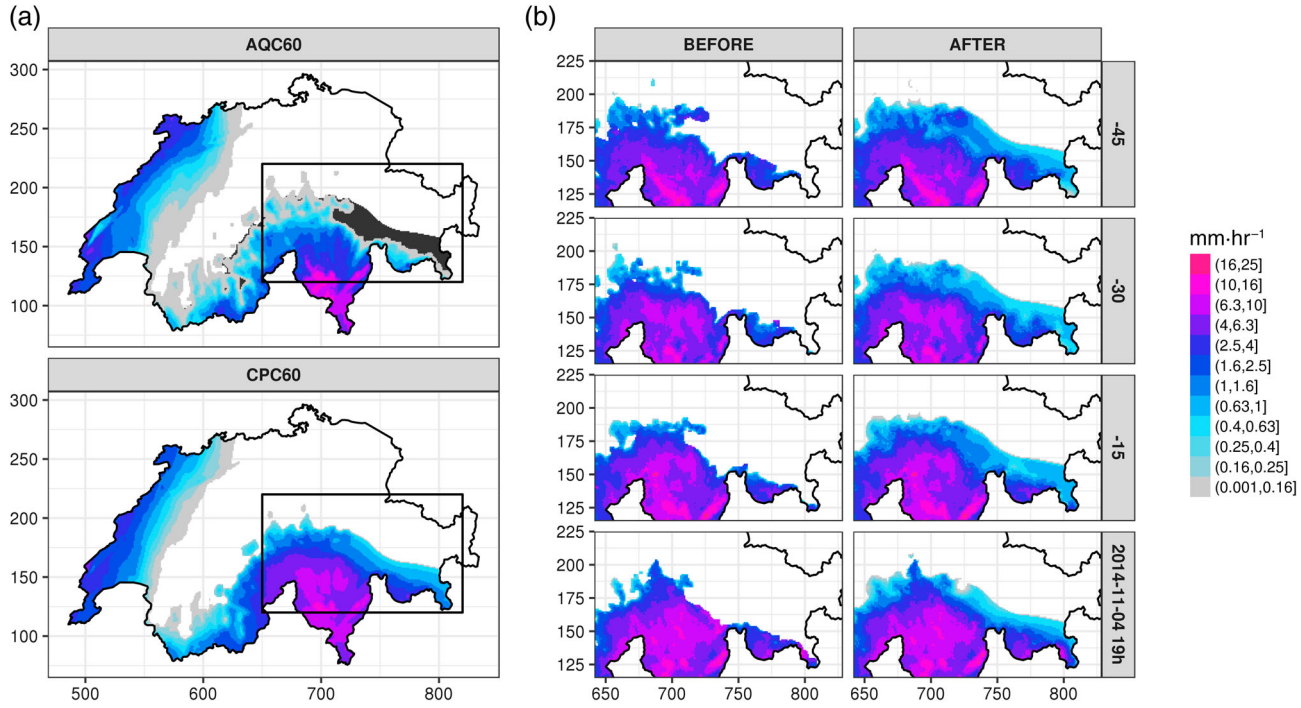

FIGURE 4 Hourly radar precipitation estimates with a dark shaded region where radar data are unavailable (a, top) and hourly blended CombiPrecip (CPC) product (a, bottom) on November 14, 2014, 1900 UTC. The respective 5 min disaggregated CPC accumulations using radar fractions only (b, left column) and using the new method (b, right column) at $t-45$, $t-30$, $t-15$ and $t-0$ min. All precipitation values are expressed in mm·hr^{-1} on a logarithmic scale

"slow" event. Precipitation moves with a speed of less than 1 km·hr^{-1}. A 20 km wide band of precipitation in the south-eastern Swiss Alps was not captured by the radar (depicted by the dark shaded region in Figure 4a, top). The disaggregation method proposed here produces visually seamless and realistic precipitation patterns in this area (Figure 4b) whereas artefacts manifesting as sharp gradients are clearly visible if the hourly precipitation is disaggregated using radar fractions only without extrapolation in locations where no radar precipitation signal is recorded.

The second example (Figure 5) shows an advective-type situation, a so-called "fast" event, on March 2, 2015, between 2100 and 2200 UTC that is characterized by scattered showers moving across Switzerland from west to east with a speed of the order of 25 km·hr^{-1}. The CPC60 product contains precipitation estimates in areas with zero precipitation in the hourly radar estimates over parts of the eastern Alps as indicated by the black region. At time step $t-30$ a distinct precipitation cell can be observed at 775 km E and 187 km N moving eastwards (not shown) followed by a second cell at the same location at $t-0$ (Figure 5b). This has an effect that the fraction of precipitation from the dark shaded region attributed at $t-30$ and $t-0$ is larger than at $t-15$, the time at which no radar signal is detected at this location. The disaggregation process is therefore temporally synchronized with the closest radar observations and is capable of seamlessly blending in with moving precipitation features.

Throughout these two illustrations, it is already shown that the novel disaggregation method produces more reliable precipitation fields since the limitation of zero accumulations and thereby related spatial artefacts is mitigated. Moreover, the local spatio-temporal variability in successive 5 min rainfall fields resembles that of real precipitation. The effort of the proposed method is basically to improve over the simple uniform distribution of the hourly precipitation to the 12 5 min accumulations and it achieves this using the presented algorithm. The superiority is demonstrated hereafter in the skill scores (Sections 4.2 and 4.3).

4.2 | Cross-validation

For each of the 1,000 hr, three non-overlapping 32 × 32 km square boxes (corresponding approximately to the largest expected size of spatial discontinuities between the hourly CPC60 and AQC60) are randomly placed in the hourly AQC precipitation field. These boxes are located within the boundaries of Switzerland and each contains at least one rain gauge from the auxiliary network. Values inside the box are set to zero in all corresponding AQC5 fields of the respective hour to imitate missing radar estimates. The disaggregation method is then performed using these AQC5 images,

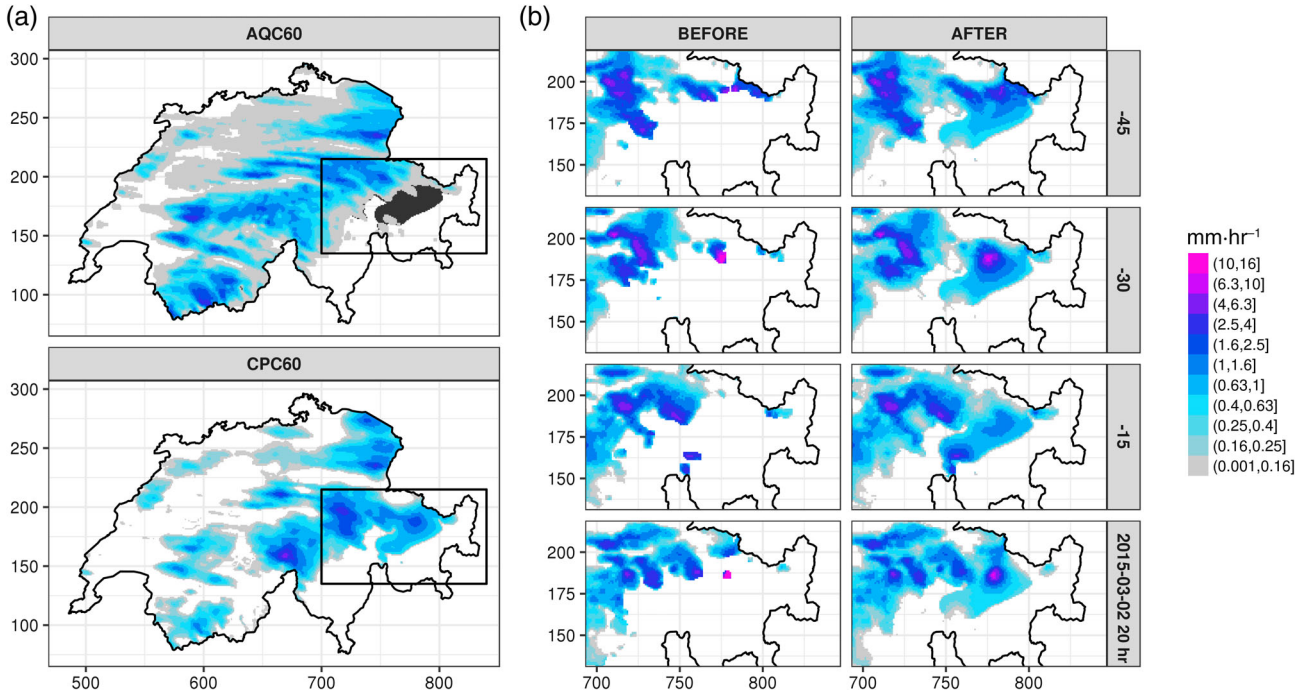

FIGURE 5 The same as Figure 4 for March 2, 2015, 2200 UTC

and the reconstructed CPC5 precipitation within the boxes (CPC5-DIS) is assessed and compared to the reference CPC5 fields (CPC5-REF) which have been computed using the standard disaggregation method as defined in Equation (1), i.e. using the radar fractions. CPC5-REF is used as a reliable reference against which the disaggregation methodology is verified. In the rest of the paper this procedure is referred to as "cross-validation". Artificially setting parts of the original AQC5 fields to zero mimics regions where radar information is unavailable. This has two advantages: on the one hand it allows us to carry out a cross-validation, which increases the robustness of the method verification, and second it allows the comparison to a larger rain gauge sample given the infrequent and isolated occurrences of regions where radar data are unavailable.

4.2.1 | Spatial properties

To assess the spatial characteristics of the reconstructed precipitation fields at different spatial scales, a fast Fourier transform is applied to the CPC5 fields at the location of the boxes. Azimuthally averaged power spectra (e.g. Pegram and Clothier, 2001) are computed for CPC5-REF, CPC5-DIS and CPC5-UNI to give the power spectral density as a function of scale. The spectra are assessed with the mean squared error (MSE) computed at each spatial scale between CPC5-DIS and CPC5-REF and compared to the benchmark (MSE between CPC5-UNI and CPC5-REF). As such, it is possible to show how strongly each scale in CPC5-DIS and CPC5-UNI is represented in the reference CPC5-REF.

Figure 6 shows the mean and spread (expressed by the interquartile range) of the fast Fourier transform distributions at each spatial scale as a simple measure of the similarities in the spatial variability contained in the 5 min precipitation fields between CPC5-REF, CPC5-DIS and CPC5-UNI. Uniformly disaggregating the hourly accumulations results in a general underestimation of the precipitation intensity in the median and interquartile range at all spatial scales for both the slow and the fast hours in the power spectra distributions compared to CPC5-REF. The distributions of the power spectra from the CPC5-DIS fields are in closer agreement with the reference fields at all spatial scales (significantly different, however, according to a Kolmogorov–Smirnov test), an indication that the CPC5-DIS fields are characterized by more coherent spatial structures with respect to CPC5-REF than the CPC5-UNI fields. Indeed, scale-dependent MSE skill scores (Figure 7) indicate a superior performance of CPC5-DIS compared to CPC5-UNI at all spatial scales. For slow hours a 50% to 80% improvement in MSE is found. For fast hours the performance gain is even larger with an improvement ranging from 50% to 90%. The relative performance gain is more pronounced for spatial scales below 2 km, i.e. near the pixel scale; however, this concerns extremely small magnitudes, which have a negligible effect. One explanation for the non-linear behaviour of the skill scores for spatial scales above 4 km could be that these are the spatial scales down to which the statistical dilation has an effective impact on the precipitation fields.

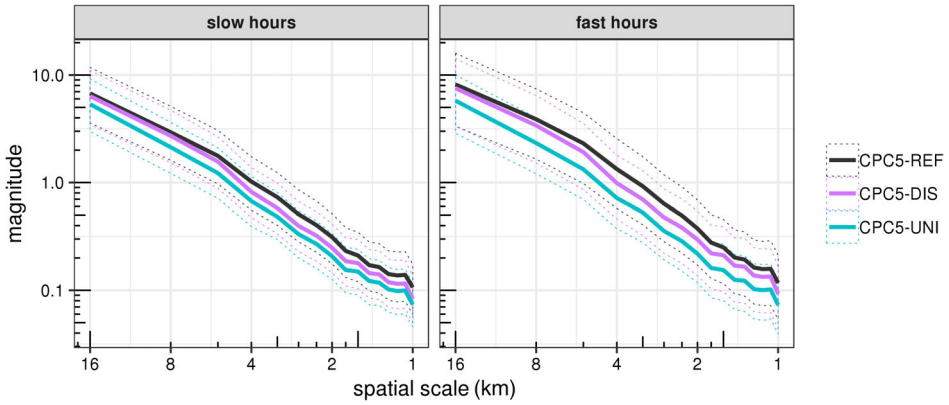

FIGURE 6 Median (solid lines) and interquartile range (dotted lines) of azimuthally averaged power spectra for slow (left) and fast (right) hours of 5 min accumulated precipitation. Grey, blue and magenta stand for the reference 5 min resolution CombiPrecip (CPC) data (CPC5-REF), uniformly distributed CPC data with 5 min resolution (CPC5-UNI) and cross-validated CPC data with 5 min resolution (CPC5-DIS) respectively. The power spectra are computed on the 32 × 32 km fields artificially blanked in the cross-validation procedure. Note the exponent 2 in km

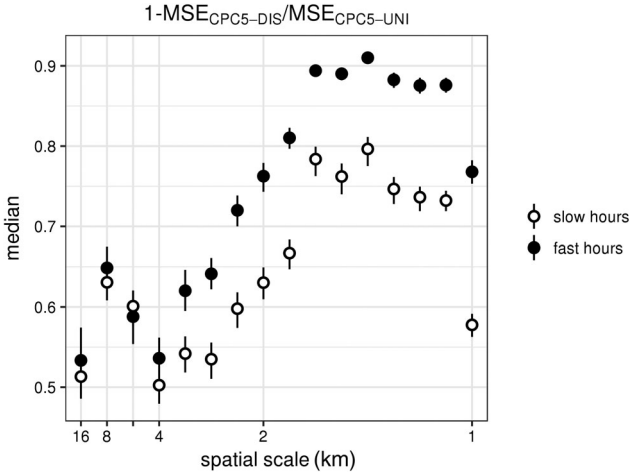

FIGURE 7 Skill score for mean squared error (MSE) conditioned on frequency bins for slow (white) and fast (black) hours. The *x* axis shows the spatial scales of the frequency bins. Points and lines designate median and 95% bootstrap confidence intervals respectively

Overall, these results suggest better performance of the new disaggregation method compared to the uniform method in terms of representativeness of the spatial precipitation structures at all spatial scales, especially for the fast hours.

4.2.2 | Temporal properties

The temporal evolution of the precipitation quantities in CPC5-DIS and CPC5-REF and their correlation constitutes a central part in the assessment of the disaggregation method. It should be remembered that the hourly accumulations are conserved at each location; therefore, differences between CPC5-REF, CPC5-DIS and the CPC5-UNI time series can be entirely attributed to differences in the sub-hourly partitioning of the precipitation accumulations.

Figure 8 reveals the predominance of very small disaggregated 5 min values, the median of the reference distribution being 0.035 for slow hours and 0.018 mm for fast hours. During fast hours the precipitation is characterized by larger values, a larger spread and there are more hours exhibiting substantial differences between the CPC5-REF and CPC5-DIS data than during slow hours. Note that expecting 5 min quantities to be correctly reproduced within 32 × 32 km boxes is a very demanding test and therefore Figure 8a should be treated as a global depiction of the 5 min precipitation distributions.

The temporal coherence of the reconstructed precipitation fields CPC5-DIS are assessed on the basis of Spearman's rank correlation co-efficients computed between the CPC5-DIS and CPC5-REF time series at each pixel within the boxes and for every hour, i.e. over the respective 12 5 min time stamps. Interestingly, the median of the Spearman's rank correlation co-efficients (Figure 8b) is slightly better for fast hours (0.7) than for slow hours (0.66). This is an indication that the method proposed in this study is able to account for moving precipitation features. According to the cumulative distribution function (CDF) in Figure 8b, approximately 70% of the time series at each pixel location have a correlation co-efficient larger than 0.5.

To relate the temporal evolution of CPC5-DIS to CPC5-UNI, absolute deviations at each 5 min time step between the CPC5-UNI and CPC5-REF time series and between the CPC5-DIS and CPC5-REF time series are shown in Figure 8c. For both slow and fast hours, absolute deviations are smaller for CPC5-DIS data than for CPC5-UNI data in terms of both median and spread.

4.3 | Rain gauges

The reliability of changes in time in the CPC5-REF and CPC5-DIS precipitation accumulations is tested using 10 min precipitation accumulations from an auxiliary rain gauge dataset. To this end the CPC5 fields (CPC5-REF and

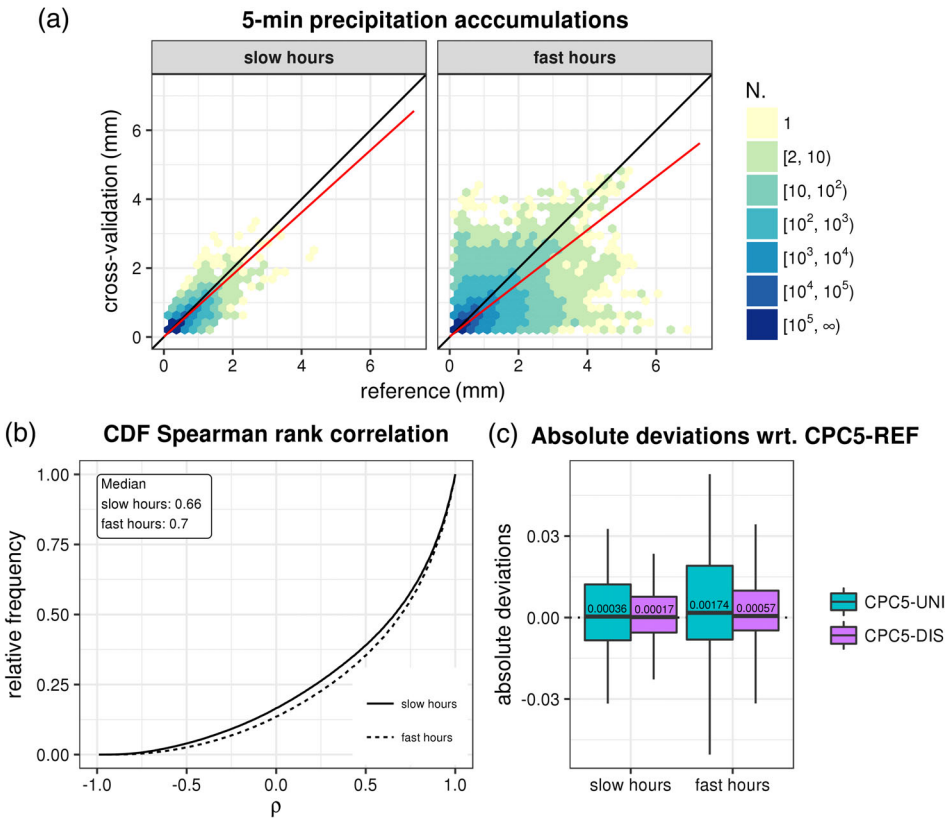

FIGURE 8 (a) Binned scatter plot of cross-validated CombiPrecip (CPC) data with 5 min resolution (CPC5-DIS) against reference 5 min resolution CPC data (CPC5-REF) for slow (left) and fast (right) hours. (b) Empirical cumulative distribution functions of the Spearman's rank correlation co-efficients between the CPC5-DIS and CPC5-REF time series at each pixel location within the 32 × 32 km boxes. The solid (dashed) line stand for slow (fast) hours. The frequency is shown in relative terms. The inset on the top left shows the median of the distributions. (c) Absolute deviations between CPC5-DIS in violet (uniformly distributed CPC data with 5 min resolution (CPC5-UNI) in turquoise) and CPC5-REF for slow and fast hours. The labels correspond to the median

CPC5-DIS) are aggregated to the temporal resolution of the rain gauge data (10 min).

Careful consideration should be given when a direct quantitative comparison between the concomitant CPC values and rain gauge data is performed on 10 min aggregation times. Such a comparison is complicated by the predominance of very small disaggregated precipitation values; the precipitation accumulation is often below the lowest discretization level of the rain gauge data (0.1 mm), making the rain gauge data often too coarse for an adequate verification of the temporal variability of the disaggregated precipitation values. Moreover, very low accumulations are affected by occasional erroneous tips of the tipping bucket. As a consequence, discrepancies and spatial sampling uncertainties between radar-based estimates and rain gauge measurements grow larger on sub-hourly time scales such as 10 min (e.g. Zawadzki, 1975; Villarini *et al.*, 2008).

In this study, regions where radar data are unavailable (extrapolated in Figure 9) are particularly interesting. However, a comparison of these results with the results from locations where the disaggregation is based on radar precipitation measurements is also of interest (radar-based in Figure 9). Therefore, a distinction between regions with radar-based and extrapolation-based disaggregation (reconstructed precipitation within the 32 × 32 square boxes) was made and the results are separately shown for the 500 slow and 500 fast hours. It should be noted that the auxiliary rain gauges tend to be sparser in the inner-Alpine regions (see Figure 1b). This should not have an effect on the results presented, however, since the boxes used for the blanking are placed exclusively where auxiliary rain gauges are present; regions exhibiting no rain gauges such as the inner Alps are *per* definition not assessed. In addition, there should be no discrepancies in the agreement between the blended and auxiliary gauge data, since the proximity of any auxiliary rain gauge to the automatic MeteoSwiss network (used for the blending process) is homogeneous across the study domain.

4.3.1 | Ten minute precipitation distributions

Rain gauge measurements are used to assess first the ability of the disaggregation to produce the correct precipitation quantities on a global scale and independently of the temporal synchronization of data pairs, i.e. whether data points with the same magnitude occur during the same time step. To this end, the empirical CDFs of the pooled 10 min rain gauge, CPC10-UNI and CPC10-DIS values were computed and are shown in Figure 9. The CDF can be used to detect whether some intensities are underestimated or overestimated. Bin sizes of 0.1 mm were used and frequencies are shown as exceedance probabilities obtained through normalization with the number of rain gauge locations and hours. The *y* axis shows the probability of exceeding a certain precipitation accumulation.

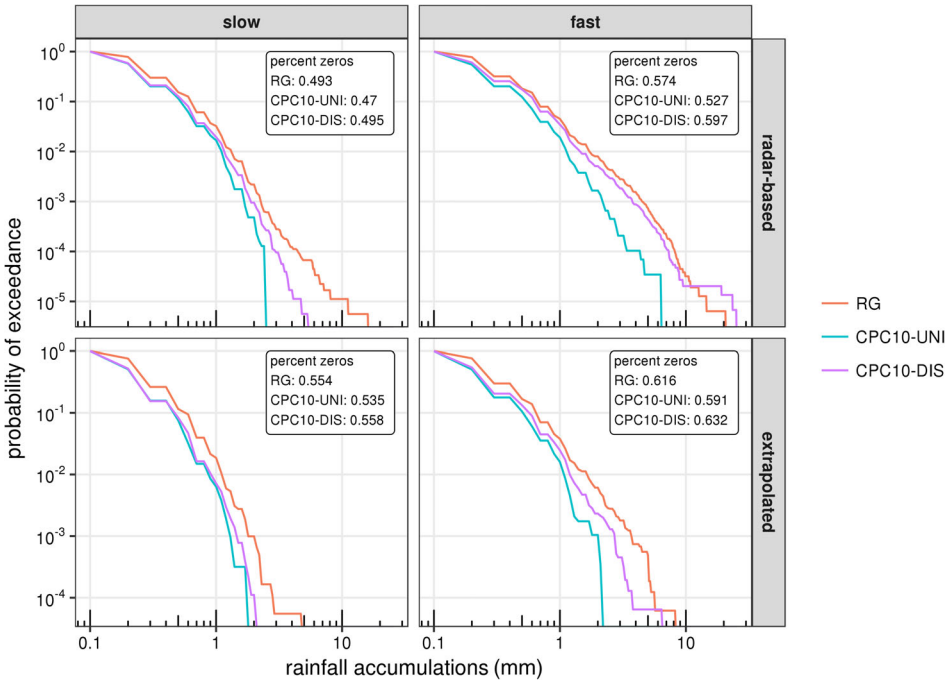

FIGURE 9 Relative cumulative distribution function of wet 10 min accumulations of rain gauge (RG), uniformly distributed CombiPrecip (CPC) data with 10 min resolution (CPC10-UNI) and cross-validated CPC data with 10 min resolution (CPC10-DIS) data. The left (right) column depicts distributions for slow (fast) hours. The top (bottom) row shows distributions from radar-based (extrapolation-based) disaggregation. The insets indicate the relative frequency of zeros in the distributions

The CPC10-UNI distributions exhibit a stronger systematic negative bias than CPC10-DIS for all accumulations, both for slow and fast hours, and independently of whether the disaggregation is radar-based or performed from extrapolations. The negative bias increases for larger precipitation accumulations and the distribution maxima are almost an order of magnitude smaller than the rain gauge maxima, e.g. 2.5 *versus* 17 mm for the radar-based slow hours.

Overall, the CPC10-DIS distributions also exhibit a systematic negative bias; however, it is smaller than for the CPC10-UNI distributions. For slow hours, the CPC10-DIS distributions are very close to the CPC10-UNI distributions although slightly closer to the rain gauge values for accumulations above 1 mm. The difference between CPC10-UNI and CPC10-DIS is largest for the fast hours.

In regions where the disaggregation is radar-based the CPC10-DIS distribution is in close agreement with the rain gauge distribution, notably for accumulations above 0.3 mm. The most extreme values also fall in the range of the rain gauge values. The overestimation of the most extreme values may be related to the radar accumulations involved in the blending process as the radar has a tendency to overestimate very large precipitation amounts. For regions where the disaggregation is based on extrapolated fractions, CPC10-DIS is also in close agreement with the rain gauge distribution (Figure 9, bottom right). This is the case especially for larger values above 1 mm.

Precipitation intermittency, i.e. 5 min periods without rainfall, is not explicitly accounted for in the disaggregation method. Zero accumulation periods are indirectly generated through extremely small accumulation values that fall below the detection threshold of the rain gauges. Here, the 10 min disaggregated data are set to zero for values below 0.1 mm for comparison with the rain gauge data. The relative frequency of zero values is shown in Figure 9. The frequencies of zeros of the CPC10-DIS data are in close agreement with the frequencies of the rain gauge distributions (performing better than the CPC10-UNI distribution).

4.3.2 | Quantification of the temporal coherence

The temporal coherence between the disaggregated 10 min CPC values and the rain gauge measurements is of central interest in this study, particularly for regions where CPC10 values are based on extrapolations. The quantification of the temporal coherence is achieved by computing the mean of the absolute deviations between the respective rain gauge and grid-value pairs (AQC10, CPC10-UNI and CPC10-DIS) across all points and all times in the 32×32 square boxes. Note that the data of all gauges are pooled together since the random placement of the boxes across the study domain led to time series of varying lengths. A measure of the difference such as the absolute deviation is well adapted in this context and allows for a stratification by rainfall intensity. Figure 10 shows the mean and interquartile range of these absolute deviations conditioned on rain gauge precipitation accumulations and shown for 500 slow and 500 fast hours.

Slow hours exhibit a non-significant difference between the uniform method and the disaggregated values. This can be expected since stationary precipitation is often characterized by low variability in the precipitation over 1 hr and therefore precipitation quantities approach a uniform

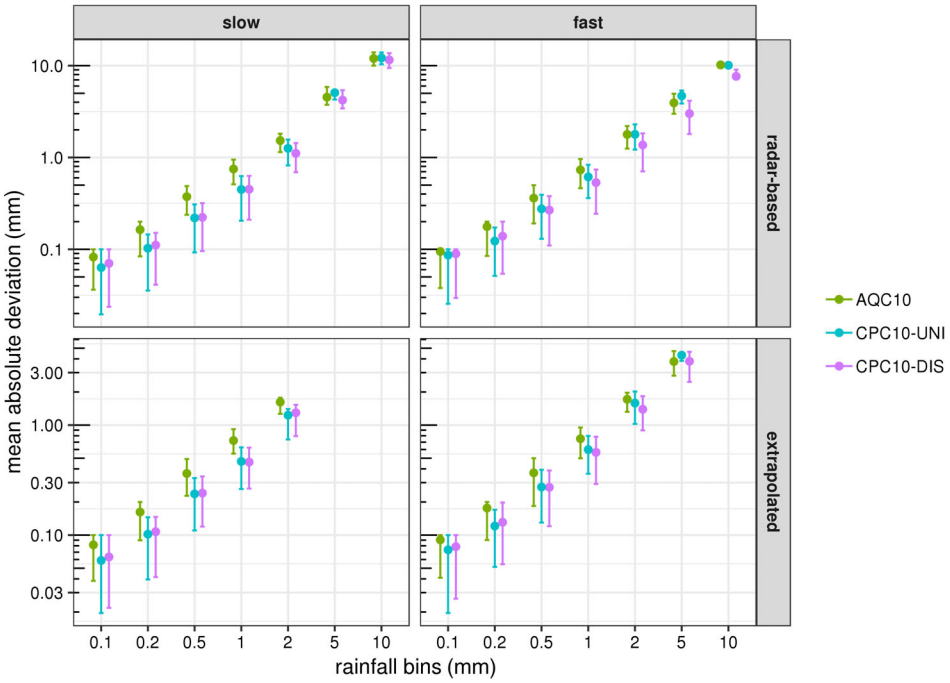

FIGURE 10 Mean absolute deviations of wet 10 min accumulations of radar (AQC10), uniformly distributed CombiPrecip (CPC) data with 10 min resolution (CPC10-UNI) and cross-validated CPC data with 10 min resolution (CPC10-DIS) conditioned on rain gauge precipitation accumulations. The left (right) column depicts results for slow (fast) hours. The top (bottom) row shows results from the radar-based (extrapolation-based) disaggregation. The bars indicate the interquartile range of the error distributions

distribution (sub-hourly temporal variability may be masked out by the discretization). For accumulations above 0.5 mm, fast hours are associated with smaller absolute deviations, more clearly distinguishable for the radar-based disaggregated data but also exhibited in the extrapolation-based disaggregated data. Although the comparison of such low values with rain gauge data is a very risky task, the quantification of the temporal coherence suggests that CPC10-DIS improves over CPC10-UNI concerning the sub-hourly partitioning of the hourly quantities for the fast hours.

5 | CONCLUSIONS

The CombiPrecip (CPC) disaggregation method is presented in this study. This is a novel approach for temporally disaggregating hourly to 5 min precipitation accumulations exclusively relying on radar precipitation estimates, specifically designed for blended precipitation products and real-time applications. In regions characterized with partial absence of radar information, the method performs the disaggregation on spatially dilated 5 min radar estimates and spatio-temporally correlated stochastic noise fields. Wherever radar information is available, the temporal disaggregation is based on the hourly 5 min radar precipitation fractions.

Spatial inconsistencies between the radar and the blended product may be caused by limited radar visibility, from smoothing inherent to the blending interpolation scheme or when the rain gauge measurements at a location where the radar observes no precipitation are different from zero. Such inconsistencies are usually accompanied by sharp precipitation gradients, artefacts that are undesired in the framework of real-time visualization of the precipitation fields. The method presented here is designed to overcome such artefacts and produces visually seamless and realistic 5 min precipitation maps on a 1 km^2 grid resolution, suitable for nowcasting applications.

In regions with no radar data availability, hourly fractions have to be estimated while conserving the hourly accumulations. These are obtained at first by spatially dilating the 5 min radar precipitation fields by means of low-pass filtering, i.e. an iterative approach is used to replace zero precipitation values gradually with the average precipitation in a 3×3 pixel box, therefore spatially extending the precipitation field with values that are naturally decreasing with distance from the edge of observed 5 min radar precipitation. At far distances, the fractions are determined stochastically, i.e. are extracted from a sequence of stochastic noise fields with spatio-temporal properties similar to those of precipitation. To ensure a seamless transition between the dilated and stochastic parts, the noise is added to the dilated precipitation but since it is extremely small the visual impact on the dilated precipitation is negligible. The effective distance of the statistical dilation is determined automatically and depends on the rate at which the values converge with the stochastic noise fields.

Visual inspection of two distinct examples demonstrates that the CPC disaggregation method is able to produce seamless 5 min precipitation fields with consistent spatio-temporal characteristics. For example, in the case of advecting precipitation and in locations where radar data are

missing, the fractions of hourly precipitation react to moving features such that the attributed precipitation is larger in close proximity to observed rainfall.

The verification of the CPC disaggregation method was performed on a set of 1,000 hr separated into slow and fast hours. Spectral analysis of the cross-validation results reveals improved spatial characteristics of the new method at all spatial scales with respect to uniformly distributed hourly accumulations. Results on the median and standard error of absolute deviations in the cross-validation time series suggest that the new method is able to represent the temporal partitioning of the rainfall data more coherently than a uniform distribution. Interestingly, the median of correlation co-efficients (Spearman) between the cross-validation and reference time series is higher for fast hours than for slow hours suggesting that the method correctly attributes hourly fractions around moving precipitation features. The comparison of the disaggregated data with an independent set of 10 min rain gauge data indicates a more faithful representation of the 10 min precipitation quantities (and per cent zeros) than for uniform quantities, especially concerning values above 1 mm and fast hours even in regions where the disaggregation relies on extrapolated fractions. Also the pairwise comparison, used to assess the temporal correlation, between the disaggregated and rain gauge values suggests an improvement over the uniform distribution for values above 1 mm and fast hours.

The CPC disaggregation method, specifically designed to resolve visual artefacts, therefore also reveals realistic and coherent disaggregated quantities in regions where radar data are missing. The high flexibility of the method makes it easily adaptable to specific demands meeting varying levels of complexity, such as the use of a more complex filter in the dilation process, the dynamic generation noise fields on spatial subsets with locally varying parameters and accounting for spatial anisotropy. This makes the method particularly useful for weather services as an advanced solution for executing disaggregations on their own products taking into consideration pragmatic problems such as measurement errors or partial absence of measurements.

ACKNOWLEDGEMENTS

The authors would like to thank two anonymous reviewers for their assistance in evaluating this paper. The authors would also like to thank MeteoGroup Schweiz AG and the concerned Swiss cantonal authorities for providing high quality rain gauge measurements. Special thanks also go to Marco Gabella, Loris Foresti, Linda Frossard and Philippe Naveau for their valuable advice and contributions that led to improvement of this paper.

ORCID

Yannick Barton https://orcid.org/0000-0003-0444-0145

REFERENCES

Beauchemin, S.S. and Barron, J.L. (1995) The computation of optical flow. *ACM Computing Surveys*, 27(3), 433–466. https://doi.org/10.1145/212094.212141.

Berenguer, M., Sempere-Torres, D. and Pegram, G.G. (2011) SBMcast–an ensemble nowcasting technique to assess the uncertainty in rainfall forecasts by Lagrangian extrapolation. *Journal of Hydrology*, 404(3–4), 226–240. https://doi.org/10.1016/j.jhydrol.2011.04.033.

Brunetti, M.T., Peruccacci, S., Antronico, L., Bartolini, D., Deganutti, A.M., Gariano, S.L., Lovine, G., Luciani, S., Luino, F., Melillo, M., Palladino, M.R., Parise, M., Rossi, M., Turconi, L., Vennari, C., Vessia, G., Viero, A. and Guzetti, F. (2015) Catalogue of rainfall events with shallow landslides and new rainfall thresholds in Italy. In: *Engineering Geology for Society and Territory, Volume 2*. Cham: Springer, pp. 1575–1579. https://doi.org/10.1007/978-3-319-09057-3_280.

Debele, B., Srinivasan, R. and Parlange, J.Y. (2007) Accuracy evaluation of weather data generation and disaggregation methods at finer timescales. *Advances in Water Resources*, 30(5), 1286–1300. https://doi.org/10.1016/j.advwatres.2006.11.009.

Germann, U., Boscacci, M., Gabella, M. and Sartori, M. (2015) Radar design for prediction in the Swiss Alps. *Meteorological Technology International*, 4, 42–45.

Germann, U., Galli, G., Boscacci, M. and Bolliger, M. (2006) Radar precipitation measurement in a mountainous region. *Quarterly Journal of the Royal Meteorological Society*, 132(618), 1669–1692. https://doi.org/10.1256/qj.05.190.

Gutierrez-Magness, A.L. and McCuen, R.H. (2004) Accuracy evaluation of rainfall disaggregation methods. *Journal of Hydrologic Engineering*, 9(2), 71–78. https://doi.org/10.1061/(ASCE)1084-0699(2004)9:2(71).

Guzzetti, F., Peruccacci, S., Rossi, M. and Stark, C.P. (2008) The rainfall intensity–duration control of shallow landslides and debris flows: an update. *Landslides*, 5(1), 3–17. https://doi.org/10.1007/s10346-007-0112-1.

Koutsoyiannis, D. (2003) Rainfall disaggregation methods: theory and applications. In: *Workshop on Statistical and Mathematical Methods for Hydrological Analysis*. Rome: Università di Roma "La Sapienza", 5270, pp. 1–23. https://doi.org/10.13140/RG.2.1.2840.8564.

Liechti, K., Panziera, L., Germann, U. and Zappa, M. (2013) The potential of radar-based ensemble forecasts for flash-flood early warning in the southern Swiss Alps. *Hydrology and Earth System Sciences*, 17(10), 3853–3869. https://doi.org/10.5194/hess-17-3853-2013.

Panziera, L., Gabella, M., Zanini, S., Hering, A., Germann, U. and Berne, A. (2016) A radar-based regional extreme rainfall analysis to derive the thresholds for a novel automatic alert system in Switzerland. *Hydrology and Earth System Sciences*, 20(6), 2317–2332. https://doi.org/10.5194/hess-20-2317-2016.

Paulat, M., Frei, C., Hagen, M. and Wernli, H. (2008) A gridded dataset of hourly precipitation in Germany: its construction,

climatology and application. *Meteorologische Zeitschrift*, 17(6), 719–732. https://doi.org/10.1127/0941-2948/2008/0332.

Pegram, G.G.S. and Clothier, A.N. (2001) High resolution space–time modelling of rainfall: the "String of Beads" model. *Journal of Hydrology*, 241(1–2), 26–41. https://doi.org/10.1016/S0022-1694(00)00373-5.

Sideris, I.V., Gabella, M., Erdin, R. and Germann, U. (2014) Real-time radar–rain-gauge merging using spatio-temporal co-kriging with external drift in the Alpine terrain of Switzerland. *Quarterly Journal of the Royal Meteorological Society*, 140(680), 1097–1111. https://doi.org/10.1002/qj.2188.

Smith, P.J., Panziera, L. and Beven, K.J. (2014) Forecasting flash floods using data-based mechanistic models and NORA radar rainfall forecasts. *Hydrological Sciences Journal*, 59(7), 1403–1417. https://doi.org/10.1080/02626667.2013.842647.

Urban Rainfall Monitoring. (n.d.). *EAWAG*. Available at: https://www.eawag.ch/en/department/sww/projects/urban-rainfall-monitoring/ [Accessed 22 July 2019].

Villarini, G., Mandapaka, P.V., Krajewski, W.F. and Moore, R.J. (2008) Rainfall and sampling uncertainties: a rain gauge perspective. *Journal of Geophysical Research*, 113(D11), 113. https://doi.org/10.1029/2007JD009214.

Vormoor, K. and Skaugen, T. (2013) Temporal disaggregation of daily temperature and precipitation grid data for Norway. *Journal of Hydrometeorology*, 14(3), 989–999. https://doi.org/10.1175/JHM-D-12-0139.1.

Westra, S., Fowler, H.J., Evans, J.P., Alexander, L.V., Berg, P., Johnson, F., Kendon, E.J., Lenderink, G. and Roberts, N.M. (2014) Future changes to the intensity and frequency of short-duration extreme rainfall. *Reviews of Geophysics*, 52(3), 522–555. https://doi.org/10.1002/2014RG000464.

Wüest, M., Frei, C., Altenhoff, A., Hagen, M., Litschi, M. and Schär, C. (2010) A gridded hourly precipitation dataset for Switzerland using rain-gauge analysis and radar-based disaggregation. *International Journal of Climatology*, 30(12), 1764–1775. https://doi.org/10.1002/joc.2025.

Zawadzki, I.I. (1975) On radar–raingage comparison. *Journal of Applied Meteorology*, 14(8), 1430–1436.

How to cite this article: Barton Y, Sideris IV, Germann U, Martius O. A method for real-time temporal disaggregation of blended radar–rain gauge precipitation fields. *Meteorol Appl*. 2020;27:e1843. https://doi.org/10.1002/met.1843